

Universal Properties of Weakly Bound Two-Neutron Halo Nuclei

Masaru Hongo^{1,2,3} and Dam Thanh Son⁴

¹*Department of Physics, University of Illinois, Chicago, Illinois 60607, USA*

²*RIKEN iTHEMS, RIKEN, Wako 351-0198, Japan*

³*Department of Physics, Niigata University, Niigata 950-2181, Japan*

⁴*Kadanoff Center for Theoretical Physics, University of Chicago, Chicago, Illinois 60637, USA*

(Dated: January 2022)

We construct an effective field theory of a two-neutron halo nucleus in the limit where the two-neutron separation energy B and the neutron-neutron two-body virtual energy ϵ_n are smaller than any other energy scale in the problem, but the scattering between the core and a single neutron is not fine-tuned, and the Efimov effect does not operate. The theory has one dimensionless coupling which formally runs to a Landau pole in the ultraviolet. We show that many properties of the system are universal in the double fine-tuning limit. The ratio of the mean-square matter radius and charge radius is found to be $\langle r_m^2 \rangle / \langle r_c^2 \rangle = Af(\epsilon_n/B)$, where A is the mass number of the core and f is a function of the ratio ϵ_n/B which we find explicitly. In particular, when $B \gg \epsilon_n$, $\langle r_m^2 \rangle / \langle r_c^2 \rangle = \frac{2}{3}A$. The shape of the $E1$ dipole strength function also depends only on the ratio ϵ_n/B and is derived in explicit analytic form. We estimate that for the ^{22}C nucleus higher-order corrections to our theory are of the order of 20% or less if the two-neutron separation energy is less than 100 keV and the s -wave scattering length between a neutron and a ^{20}C nucleus is less than 2.8 fm.

Introduction.—Neutron-rich nuclei near the neutron drip line are at the forefront of modern nuclear physics. Some of the most exotic examples are two-neutron halo nuclei, consisting of a relatively tightly bound core and two weakly bound neutrons, e.g., ^6He , ^{11}Li , and ^{22}C . These nuclei are called “Borromean,” i.e., bound states of three objects which would fall apart when one is removed [1].

In this Letter, we develop an effective field theory (EFT) that can describe Borromean two-neutron halo nuclei in the limit of very small two-neutron separation energy B . The impetus to the construction of this theory is the observation of the halo nucleus ^{22}C with a matter radius found to be as large as 5.4(9) fm [2] which requires a small B : $B < 100$ keV [3]. A later experiment [4] yields a smaller matter radius—3.44(8) fm—relaxing the upper limit to $B < 400$ keV, but if one incorporates the information about the neutron-core scattering [5], the upper limit is reduced to $B < 180$ keV [6]. So ^{22}C is likely the least bound among the known Borromean nuclei.

Our EFT requires two fine-tunings: We assume that the neutron-neutron s -wave scattering length a is unnaturally large and the two-neutron separation energy of the halo nucleus is unnaturally small. In other words, the n - n two-body virtual energy $\epsilon_n = \hbar^2/(m_n a^2) \approx 120$ keV (here, m_n is the neutron mass) and the binding energy B of the core with two neutrons are assumed to be smaller than all other energy scales in the problem. We do not presume any hierarchy between these two energies.

Some previous attempts to apply the EFT philosophy to two-neutron halo nuclei [6, 7] rely on the existence of a near-threshold resonance in the core-neutron subsystem and the three-body Efimov effect [8]. This resonance seems to be absent in the case of ^{22}C , where experiment points to a rather small $^{20}\text{C}+n$ scattering length [5]. The theory developed in this Letter is designed to address this situation. It may also be a reasonable starting point

for a description of the $^3\text{He}^4\text{He}_2$ molecular trimer [9], whose binding energy (~ 10 – 15 mK) [10] is somewhat smaller than the energy scale set by the ^3He – ^4He scattering length (around 50 mK [11]).

The EFT, to be described, contains two relevant parameters and one dimensionless coupling. The two relevant parameters correspond to the two fine-tunings. The dimensionless coupling g can be interpreted as the probability that a halo nucleus splits into a core and a two-neutron dimer (“dineutron”), and it runs logarithmically with energy, reaching formally a Landau pole in the ultraviolet (UV) and zero in the infrared (IR) [12]. All other coupling constants are irrelevant and can be neglected in leading-order calculation.

Using the EFT, one can compute many physical quantities. In particular, we compute the ratio of the mean-square matter radius and charge radius. The result is particularly simple in the limit of infinite neutron-neutron scattering length:

$$\frac{\langle r_m^2 \rangle}{\langle r_c^2 \rangle} = \frac{2}{3}A, \quad (1)$$

where A is the mass number of the core. We also obtain a fully analytic expression for the $E1$ dipole strength function, Eqs. (29) and (30).

All calculations in this Letter are performed under the assumption that the core and the neutron are pointlike particles. To translate our results to the realistic nuclei, one needs account for the charge and matter distribution inside the core and the neutrons. In addition, effects from irrelevant terms in the effective Lagrangian may need to be taken into account.

The effective field theory.—We first write down the effective Lagrangian for the neutron sector. Denoting the

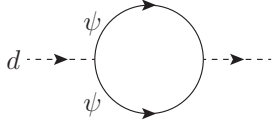


FIG. 1. The self-energy of the dimer.

neutron by ψ_α , $\alpha = \uparrow, \downarrow$ being the spin index,

$$\mathcal{L}_n = \sum_\sigma \psi_\sigma^\dagger \left(i\partial_t + \frac{\nabla^2}{2m_n} \right) \psi_\sigma + c_0 \psi_\uparrow^\dagger \psi_\downarrow^\dagger \psi_\downarrow \psi_\uparrow. \quad (2)$$

From now on, we set $m_n = 1$. Using a Hubbard-Stratonovich transformation, the Lagrangian can be transformed into

$$\mathcal{L}_n = \sum_\sigma \psi_\sigma^\dagger \left(i\partial_t + \frac{\nabla^2}{2} \right) \psi_\sigma - \frac{1}{c_0} d^\dagger d + \psi_\uparrow^\dagger \psi_\downarrow^\dagger d + d^\dagger \psi_\downarrow \psi_\uparrow. \quad (3)$$

Computing the self-energy of the dimer d , which, in the nonrelativistic theory, is exactly given by the one-loop diagram in Fig. 1, we find the full dimer propagator

$$D(p) = -\frac{4\pi}{\sqrt{-p_0 + \frac{\mathbf{p}^2}{4} - \frac{1}{a}}}, \quad (4)$$

where a denotes the s -wave scattering length given by

$$\frac{1}{4\pi a} = -\frac{1}{c_0} + \int \frac{d\mathbf{q}}{(2\pi)^3} \frac{1}{\mathbf{q}^2}. \quad (5)$$

The integral on the right-hand side linearly diverges in the UV and is proportional to the UV cutoff. The fine-tuning of c_0 leads to an unnaturally large scattering length a . Note that the UV behavior of the dimer propagator is different from that of a free field. In fact, the UV behavior corresponds to a field of dimension 2: $[d] = 2$ [13] [14].

To construct the EFT describing the halo nucleus, we add into the theory a field ϕ describing the core and h describing the halo nucleus. They can be either bosonic or fermionic. The effective Lagrangian is now [15]

$$\mathcal{L} = h^\dagger \left(i\partial_t + \frac{\nabla^2}{2m_h} + B \right) h + \phi^\dagger \left(i\partial_t + \frac{\nabla^2}{2m_\phi} \right) \phi + g(h^\dagger \phi d + \phi^\dagger d^\dagger h) + \mathcal{L}_n + \text{counterterms}, \quad (6)$$

where $m_\phi = Am_n$ and $m_h = (A+2)m_n$ are the masses of the core and the halo nucleus, respectively. As $[d] = 2$ and $[\phi] = [\psi] = \frac{3}{2}$, the dimension of the interaction $h^\dagger \phi d$ is 5, which means that g is dimensionless. One can check that terms not included in Eq. (6) are all irrelevant, since they are accompanied by more fields or derivatives. One can compute the beta function for g [16]:

$$\frac{\partial g}{\partial \ln E} = \beta(g) = \frac{2}{\pi} \left(\frac{A}{A+2} \right)^{3/2} g^3. \quad (7)$$

The solution to this equation is

$$g^2(E) = \frac{\pi}{4} \left(\frac{A+2}{A} \right)^{3/2} \frac{1}{\ln \frac{E_0}{E}}, \quad (8)$$

where E_0 is the energy of the Landau pole. Because of the properties of the nonrelativistic theory, our subsequent calculations can be done to all orders in g^2 .

One can arrive at the effective Lagrangian (6) by starting from a theory where the core ϕ and the resonantly interacting neutron are coupled to each other by a contact interaction $C_0 \phi^\dagger d^\dagger d \phi$, with a UV cutoff at the Landau pole scale. Through a Hubbard-Stratonovich transformation, one introduces an auxiliary field h with the coupling $h^\dagger d \phi + \text{H.c.}$ Integrating out degrees of freedom in a energy shell between E_0 and $E_1 < E_0$, one generates a kinetic term for h and arrive to Eq. (6) [17].

Charge and matter radii.—We now proceed to extract physical observables from the Lagrangian (6). The mean-square (rms) charge radius (the rms of the deviation of the coordinates of the core from the center of mass [18]) can be extracted from the electric form factor of the halo nucleus: $F(\mathbf{k}) = 1 - \frac{1}{6}k^2 \langle r_c^2 \rangle + O(k^4)$ [recall that $F(\mathbf{k})$ is a Fourier transform of the charge density]. The electric form factor is given by the Feynman diagram in Fig. 2; it is proportional to g^2 , and by dimensional analysis one should have $\langle r_c^2 \rangle = g^2 B^{-1} f(\beta)$, where we introduce the dimensionless parameter

$$\beta = \frac{1}{-a\sqrt{B}} = \sqrt{\frac{\epsilon_n}{B}}, \quad (9)$$

where $\epsilon_n = 1/a^2$ (we assume $a < 0$). Computing the Feynman diagram [16], we find [19]

$$\langle r_c^2 \rangle = \frac{4}{\pi} \frac{A^{1/2}}{(A+2)^{5/2}} \frac{g^2}{B} f_c(\beta), \quad (10)$$

where

$$f_c(\beta) = \begin{cases} \frac{1}{1-\beta^2} - \frac{\beta \arccos \beta}{(1-\beta^2)^{3/2}}, & \beta < 1, \\ -\frac{1}{\beta^2-1} + \frac{\beta \operatorname{arccosh} \beta}{(\beta^2-1)^{3/2}}, & \beta > 1. \end{cases} \quad (11)$$

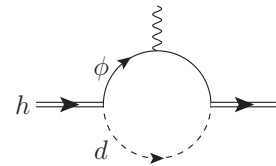


FIG. 2. The Feynman diagram determining the charge form factor of the halo nucleus. The double line represents the halo nucleus, the single line—the core, and the dotted line—the neutron dimer, whose propagator is given in Eq. (4).

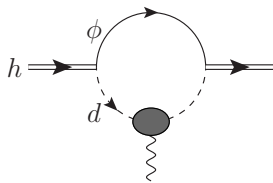


FIG. 3. The Feynman diagram determining the “neutron form factor” of the halo nucleus.

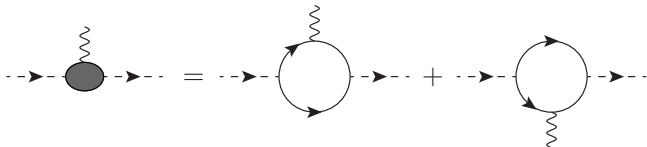


FIG. 4. The effective vertex of the dimer-photon coupling.

One can further define the “neutron radius” by imagining that there is a U(1) gauge boson coupled to the neutrons outside the core [20], which describes the spatial size of the dineutron distribution. The Feynman diagram determining the form factor of the halo nucleus with respect to this “neutron-number photon” is drawn in Fig. 3, where the effective coupling of the dimer to the photon is as in Fig. 4.

The neutron radius is then calculated to be [16]

$$\langle r_n^2 \rangle = \frac{g^2}{\pi B} \left(\frac{A}{A+2} \right)^{3/2} \left[f_n(\beta) + \frac{A}{A+2} f_c(\beta) \right], \quad (12)$$

where $f_c(\beta)$ is as in Eq. (11) and

$$f_n(\beta) = \begin{cases} \frac{1}{\beta^3} \left[\pi - 2\beta + (\beta^2 - 2) \frac{\arccos \beta}{\sqrt{1 - \beta^2}} \right], & \beta < 1, \\ \frac{1}{\beta^3} \left[\pi - 2\beta + (\beta^2 - 2) \frac{\operatorname{arccosh} \beta}{\sqrt{\beta^2 - 1}} \right], & \beta > 1. \end{cases} \quad (13)$$

Both $f_c(\beta)$ and $f_n(\beta)$ are continuous at $\beta = 1$ and have the following asymptotics at small and large values of the argument:

$$f_c(0) = 1, \quad f_n(0) = \frac{1}{3}, \quad (14)$$

$$f_c(\beta) = \frac{\ln \beta}{\beta^2}, \quad f_n(\beta) = \frac{\ln \beta}{\beta^2}, \quad \beta \rightarrow \infty. \quad (15)$$

From the charge radius and the neutron radius one can compute other radii—the mean-square matter radius $\langle r_m^2 \rangle$, the neutron-neutron distance $\langle r_{nn}^2 \rangle$, and the core-neutron distance $\langle r_{cn}^2 \rangle$ [21]:

$$\langle r_m^2 \rangle = \frac{2}{A+2} \langle r_n^2 \rangle + \frac{A}{A+2} \langle r_c^2 \rangle, \quad (16)$$

$$\langle r_{nn}^2 \rangle = 4 \langle r_n^2 \rangle - A^2 \langle r_c^2 \rangle, \quad (17)$$

$$\langle r_{cn}^2 \rangle = \langle r_n^2 \rangle + (A+1) \langle r_c^2 \rangle. \quad (18)$$

When ϵ_n is fixed, these radii depend on B in the following way. When $B \gg \epsilon_n$, the coupling g is set at the scale B , and $\langle r^2 \rangle \sim 1/[B \ln(E_0/B)]$. When $B \ll \epsilon_n$, g is frozen at the scale ϵ_n , and the radii grow logarithmically as $B \rightarrow 0$: $\langle r^2 \rangle \sim \ln(\epsilon_n/B)$, which is a known result [22].

Note that, due to the running of the coupling g , the results for the radii are not truly “universal”: They cannot be expressed solely in terms of low-energy observables—the three-body binding energy B and the neutron-neutron scattering length a . Instead, they depend logarithmically on the UV cutoff through the coupling g . However, the dependence on g disappears when one computes the ratios of the radii. For example, the ratio of the rms matter and charge radii is

$$\frac{\langle r_m^2 \rangle}{\langle r_c^2 \rangle} = \frac{A}{2} \left[1 + \frac{f_n(\beta)}{f_c(\beta)} \right], \quad (19)$$

while the ratio of the core-neutron and neutron-neutron distances is

$$\frac{\langle r_{cn}^2 \rangle}{\langle r_{nn}^2 \rangle} = \frac{1}{4} + \frac{A+2}{4A} \frac{f_c(\beta)}{f_n(\beta)}. \quad (20)$$

In the two extreme limits $B \gg \epsilon_n$ and $B \ll \epsilon_n$, these ratios become, respectively,

$$\frac{\langle r_m^2 \rangle}{\langle r_c^2 \rangle} = \begin{cases} \frac{2}{3}A, & B \gg \epsilon_n, \\ A, & B \ll \epsilon_n, \end{cases} \quad (21)$$

$$\frac{\langle r_{cn}^2 \rangle}{\langle r_{nn}^2 \rangle} = \begin{cases} 1 + \frac{3}{2A}, & B \gg \epsilon_n, \\ \frac{A+1}{2A}, & B \ll \epsilon_n. \end{cases} \quad (22)$$

One notes, however, that f_n/f_c reaches its large- β limit very slowly. For example, the ratio of the matter and charge mean-square radii does not deviate more than 10% from its $B \gg \epsilon_n$ asymptotics unless B is less than about $\frac{1}{3}\epsilon_n$ (~ 40 keV).

The dipole strength function.—The dipole strength function can also be conveniently computed from EFT. It is defined as

$$\frac{dB(E1)}{d\omega}(\omega) = \sum_n |\langle n | \mathcal{M} | 0 \rangle|^2 \delta(E_n - E_0 - \omega), \quad (23)$$

where $|0\rangle$ is the ground state of the halo, the sum is taken over all excited states $|n\rangle$, and \mathcal{M} is the dipole operator,

$$\mathcal{M} = \sqrt{\frac{3}{4\pi}} Ze(\mathbf{r}_c - \mathbf{R}_{c.m.}), \quad (24)$$

where \mathbf{r}_c is the coordinates of the core and $\mathbf{R}_{c.m.}$ of the center of mass. By noting that

$$\frac{\partial}{\partial t} \mathcal{M} = \sqrt{\frac{3}{4\pi}} \mathbf{J}, \quad (25)$$

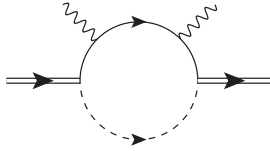


FIG. 5. The Feynman diagram for the $E1$ dipole strength function.

where \mathbf{J} is the total electric current, one can rewrite the dipole strength function as

$$\frac{dB(E1)}{d\omega} = \frac{3}{4\pi} \frac{1}{\omega^2} \sum_n |\langle n | \mathbf{J} | 0 \rangle|^2 \delta(E_n - E_0 - \omega) \quad (26)$$

and express it as the imaginary part of a two-point Green's function of the current operator:

$$\frac{dB(E1)}{d\omega} = -\frac{3}{4\pi} \frac{1}{\pi\omega^2} \text{Im} G_{JJ}(\omega), \quad (27)$$

where

$$iG_{JJ}(\omega) = \int dt e^{i\omega t} \langle 0 | T \mathbf{J}(t) \mathbf{J}(0) | 0 \rangle. \quad (28)$$

The problem is now similar to that of deep inelastic scattering in quantum chromodynamics [23]. Computing the Feynman diagram in Fig. 5, we find [16]

$$\frac{dB(E1)}{d\omega} = \frac{3}{4\pi} Z^2 e^2 \frac{12g^2}{\pi} \frac{A^{1/2}}{(A+2)^{5/2}} \frac{(\omega-B)^2}{\omega^4} \times f_{E1} \left(\frac{1}{-a\sqrt{\omega-B}} \right), \quad (29)$$

where

$$f_{E1}(x) = 1 - \frac{8}{3}x(1+x^2)^{3/2} + 4x^2 \left(1 + \frac{2}{3}x^2 \right). \quad (30)$$

The formula is more complicated than the formula for one-neutron halo nuclei [24] but is still explicit.

One can check that the $E1$ dipole strength satisfies the sum rule

$$\int_0^\infty d\omega \frac{dB(E1)}{d\omega} = \frac{3}{4\pi} Z^2 e^2 \langle r_c^2 \rangle, \quad (31)$$

with the charge radius given by Eq. (10). The energy-weighted sum rule

$$\int_0^\infty d\omega \omega \frac{dB(E1)}{d\omega} = \frac{3}{4\pi} Z^2 e^2 \frac{3}{A(A+2)} \quad (32)$$

is also valid if the logarithmic divergence of the integral on the left-hand side is regularized by a UV cutoff at the energy of the Landau pole. The two sum rules are

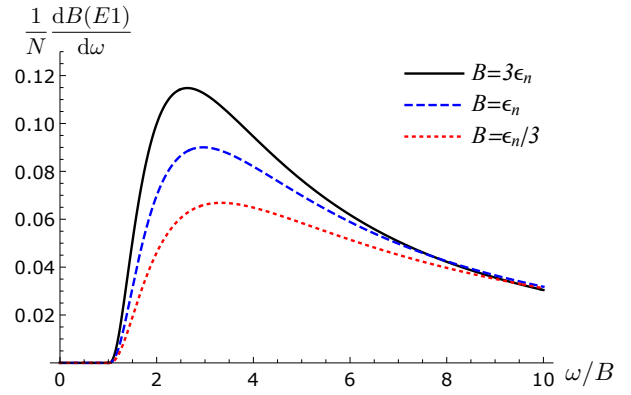


FIG. 6. The $E1$ dipole strength function, plotted as function of ω/B , for $B = 3\epsilon_n$, $B = \epsilon_n$, and $B = \frac{1}{3}\epsilon_n$. The functions are so normalized by N that the area under the theoretical curve, extended to $\omega/B = \infty$, is 1.

nontrivial checks of the self-consistency of our theoretical approach. The predicted shape of the $E1$ dipole strength is plotted in Fig. 6 as a function of ω/B for various values of β . One sees that the weight of the dipole strength shifts to larger ω/B as B/ϵ_n decreases.

Applicability to real systems.—The theory described above is applicable when the binding energy of the halo B and the n - n two-body virtual energy ϵ_n are smaller than any other energy scales in the problem. In the real world, $\epsilon_n \approx 0.12$ MeV is indeed small. For ${}^6\text{He}$ and ${}^{11}\text{Li}$, the two-neutron separation energy somewhat larger (0.975 and 0.369 MeV, respectively); in addition, the existence of near-threshold resonances in the ${}^5\text{He}$ and ${}^{10}\text{Li}$ subsystem makes the applicability of our theory doubtful.

Nevertheless, let us try to compare our results with existing experimental data and previous theoretical calculations. For ${}^6\text{He}$, Eq. (19) predicts that $\langle r_m^2 \rangle / \langle r_c^2 \rangle \approx 0.686A$. In Ref. [25], it has been argued that the data for ${}^6\text{He}$ fit the formula $\langle r_m^2 \rangle / \langle r_c^2 \rangle = 0.862A$, which the authors derived approximately. Our value is off by about 20%. For ${}^{11}\text{Li}$, we compare our results with those of Ref. [7], where $B = 247$ keV and $\epsilon_n = 116.04$ keV were used. Setting the logarithm in Eq. (8) to 1, we find $\sqrt{\langle r_c^2 \rangle} = 0.86$ fm and $\sqrt{\langle r_n^2 \rangle} = 4.7$ fm, near the center of the error bands predicted for large energies of the ${}^{10}\text{Li}$ resonance. The opening angle θ_{nn} (defined as the vertex angle of the isosceles triangle with sides $\sqrt{\langle r_{cn}^2 \rangle}$, $\sqrt{\langle r_{cn}^2 \rangle}$, and $\sqrt{\langle r_{nn}^2 \rangle}$) is close to 60° and is again within the error band. However, for the reasons listed above, it is possible that the EFT provides only a qualitative guide for ${}^{11}\text{Li}$.

The theory presented here may be quantitatively useful for the ${}^{22}\text{C}$ nucleus if its two-neutron separation energy is indeed as small as 100 keV [3]. A correction to the EFT comes from the scattering between the core and one neutron, parametrized by the irrelevant dimension-6 term $a_{cn} \phi^\dagger \psi^\dagger \psi \phi$. The contributions from this term to physi-

cal quantities should be suppressed by $a_{cn}(2m_n B)^{1/2}$ relative to the leading-order results, where a_{cn} is the core-neutron scattering length. Experiment [5] indicates that $|a_{cn}| < 2.8$ fm, so this factor is ≤ 0.2 (0.25 or 0.4 if the upper limit on B is taken as 180 or 400 keV, respectively). Another dimension-6 operator, $d^\dagger(i\partial_t + \frac{1}{4}\nabla^2)d$, has its coefficient fixed by the effective range of the s -wave neutron-neutron scattering; its effect is expected to be similarly suppressed. Other terms, e.g., $h^\dagger\nabla\phi\nabla d$, have dimension 7 and higher and should be more suppressed. Corrections from higher-order operators should be computable within effective field theory. The presence of the ${}^5\text{He}$ p -wave resonance can be taken into account by adding the corresponding field [26]. The present work is expected to open a potential direction to a quantitative study of the halo nuclei in addition to their universal properties. For the ${}^3\text{He}^4\text{He}_2$ trimers we expect corrections from ${}^3\text{He}^4\text{He}$ scattering to be relatively large: $(2\mu B)^{1/2}|a_{34}| \sim 0.5$ (where μ is the reduced mass of the ${}^3\text{He}^4\text{He}$ system and $a_{34} \approx -17$ Å is the ${}^3\text{He}^4\text{He}$ scatter-

ing length [11]). Indeed, experiment and quantum Monte Carlo simulations [27, 28] seem to imply substantially smaller values for the ratio $\langle r_{cn}^2 \rangle / \langle r_{nn}^2 \rangle$ compared the one given in Eq. (20).

ACKNOWLEDGMENTS

The authors thank Dario Bressanini, Reinhardt Dörner, Maksim Kunitski, and especially Hans-Werner Hammer for discussions. D. T. S. is supported, in part, by the U.S. Department of Energy Grant No. DE-FG02-13ER41958 and a Simons Investigator grant from the Simons Foundation. M. H. is supported by the U.S. Department of Energy, Office of Science, Office of Nuclear Physics under Grant No. DE-FG0201ER41195 and partially by RIKEN iTHEMS Program (in particular, iTHEMS Non-Equilibrium Working Group and Mathematical Physics Working Group).

-
- [1] M. V. Zhukov, B. V. Danilin, D. V. Fedorov, J. M. Bang, I. J. Thompson, and J. S. Vaagen, Bound state properties of Borromean halo nuclei: ${}^6\text{He}$ and ${}^{11}\text{Li}$, *Phys. Rep.* **231**, 151 (1993).
- [2] K. Tanaka, T. Yamaguchi, T. Suzuki, T. Ohtsubo, M. Fukuda, *et al.*, Observation of a Large Reaction Cross Section in the Drip-Line Nucleus ${}^{22}\text{C}$, *Phys. Rev. Lett.* **104**, 062701 (2010).
- [3] B. Acharya, C. Ji, and D. R. Phillips, Implications of a matter-radius measurement for the structure of Carbon-22, *Phys. Lett. B* **723**, 196 (2013), arXiv:1303.6720.
- [4] Y. Togano *et al.*, Interaction cross section study of the two-neutron halo nucleus ${}^{22}\text{C}$, *Phys. Lett. B* **761**, 412 (2016).
- [5] S. Mosby *et al.*, Search for ${}^{21}\text{C}$ and constraints on ${}^{22}\text{C}$, *Nucl. Phys.* **A909**, 69 (2013), arXiv:1304.4507.
- [6] H.-W. Hammer, C. Ji, and D. R. Phillips, Effective field theory description of halo nuclei, *J. Phys. G* **44**, 103002 (2017), arXiv:1702.08605.
- [7] D. L. Canham and H.-W. Hammer, Universal properties and structure of halo nuclei, *Eur. Phys. J. A* **37**, 367 (2008), arXiv:0807.3258.
- [8] P. Naidon and S. Endo, Efimov physics: A review, *Rep. Prog. Phys.* **80**, 056001 (2017), arXiv:1610.09805.
- [9] B. D. Esry, C. D. Lin, and C. H. Greene, Adiabatic hyperspherical study of the helium trimer, *Phys. Rev. A* **54**, 394 (1996).
- [10] See, e.g., Ref. [28] for a compilation of theoretical predictions.
- [11] Y. Uang and W. C. Stwalley, The possibility of a ${}^4\text{He}_2$ bound state, effective range theory, and very low energy He-He scattering, *J. Chem. Phys.* **76**, 5069 (1982).
- [12] In practice, the running is limited in the UV by the UV cutoff and in the IR by ϵ_n or B , whichever is larger.
- [13] Y. Nishida and D. T. Son, Nonrelativistic conformal field theories, *Phys. Rev. D* **76**, 086004 (2007), arXiv:0706.3746.
- [14] In our convention, the dimension of momentum is 1 and energy is 2.
- [15] This Lagrangian was, in essence, previously considered in Ref. [29] for the case of a three-body resonance, i.e., when the three-body binding energy B is negative.
- [16] See Supplementary Material for details.
- [17] In this scenario, the halo nucleus is bound by the three-body force. One should note, however, that the effective Lagrangian is valid irrespective of the nature of the microscopic force responsible for the binding of the halo nucleus.
- [18] What we call here the mean-square charge radius should be understood, for real nuclei, as the difference between the mean-square point-proton radii of the halo and core nuclei. Similarly, what is later called the mean-square matter radius is for real nuclei $\langle r_m^2 \rangle_h - \frac{A-2}{A}\langle r_m^2 \rangle_c$, where $\langle r_m^2 \rangle_h$ and $\langle r_m^2 \rangle_c$ are the mean-square matter radii of the halo and the core, respectively.
- [19] In subsequent formulas, g is the renormalized coupling in the on-shell renormalization scheme.
- [20] This can be done by coupling a gauge field to $B - \frac{A}{Z}Q$, where B is the baryon charge, Q is the electric charge, and Z and A are the atomic and mass numbers, respectively, of the core.
- [21] Using the positions of the core \mathbf{r}_c and two neutrons \mathbf{r}_1 and \mathbf{r}_2 , we define $r_m^2 \equiv \frac{1}{A+2}(A\mathbf{r}_c^2 + \mathbf{r}_1^2 + \mathbf{r}_2^2)$, $r_{nn}^2 \equiv (\mathbf{r}_1 - \mathbf{r}_2)^2$, and $r_{cn}^2 \equiv \frac{1}{2}((\mathbf{r}_1 - \mathbf{r}_c)^2 + (\mathbf{r}_2 - \mathbf{r}_c)^2)$.
- [22] D. V. Fedorov, A. S. Jensen, and K. Riisager, Three-body halos: Gross properties, *Phys. Rev. C* **49**, 201 (1994).
- [23] M. E. Peskin and D. V. Schroeder, *An Introduction to Quantum Field Theory* (Addison-Wesley, Reading, 1995).
- [24] S. Typel and G. Baur, Effective-Range Approach and Scaling Laws for Electromagnetic Strength in Neutron-Halo Nuclei, *Phys. Rev. Lett.* **93**, 142502 (2004), arXiv:nucl-th/0406068.

- [25] B. V. Danilin, S. N. Ershov, and J. S. Vaagen, Charge and matter radii of Borromean halo nuclei: The ${}^6\text{He}$ nucleus, *Phys. Rev. C* **71**, 057301 (2005).
- [26] C. A. Bertulani, H. W. Hammer, and U. Van Kolck, Effective field theory for halo nuclei: Shallow p-wave states, *Nucl. Phys. A* **712**, 37 (2002), [arXiv:nucl-th/0205063](#).
- [27] J. Voitgtsberger *et al.*, Imaging the structure of the trimer systems ${}^4\text{He}_3$ and ${}^3\text{He}^4\text{He}_2$, *Nat. Commun.* **5**, 5765 (2014).
- [28] D. Bressanini, The Structure of the Asymmetric Helium Trimer ${}^3\text{He}^4\text{He}_2$, *J. Phys. Chem. A* **118**, 6521 (2014).
- [29] D. T. Son, M. Stephanov, and H.-U. Yee, Fate of Multiparticle Resonances: From Q -Balls to ${}^3\text{He}$ Droplets, (2021), [arXiv:2112.03318](#).

— Supplementary Material —

Universal Properties of Weakly Coupled Two-Neutron Halo Nuclei

Masaru Hongo and Dam Thanh Son

S1. FIELD THEORY: FEYNMAN RULES, RENORMALIZATION

In terms of the bare fields and bare couplings, the Lagrangian of the theory of the halo nucleus is

$$\mathcal{L} = h_0^\dagger \left(i\partial_t + \frac{\nabla^2}{2m_h} + B_0 \right) h_0 + \phi^\dagger \left(i\partial_t + \frac{\nabla^2}{2m_\phi} \right) \phi + g_0 (h_0^\dagger \phi d + \phi^\dagger d^\dagger h_0) + \mathcal{L}_n. \quad (\text{S1})$$

where \mathcal{L}_n is written in Eq. (2). Define the renormalized halo field h and renormalized coupling g :

$$h_0 = \sqrt{Z_h} h, \quad g = \sqrt{Z_h} g_0, \quad (\text{S2})$$

the Lagrangian is

$$\mathcal{L} = Z_h h^\dagger \left(i\partial_t + \frac{\nabla^2}{2m_h} + B_0 \right) h + \phi^\dagger \left(i\partial_t + \frac{\nabla^2}{2m_\phi} \right) \phi + g (h^\dagger \phi d + \phi^\dagger d^\dagger h) + \mathcal{L}_n. \quad (\text{S3})$$

The Feynman rules are as follows. The dimer propagator is

$$iD(p) = -4i\pi f_a \left(\frac{\mathbf{p}^2}{4} - p_0 - i\epsilon \right), \quad (\text{S4})$$

where we introduce the notation

$$f_a(x) = \frac{1}{\sqrt{x - \frac{1}{a}}}. \quad (\text{S5})$$

The core propagator is

$$iG_\phi(p) = \frac{i}{p_0 - \frac{\mathbf{p}^2}{2m_\phi} + i\epsilon}, \quad (\text{S6})$$

and the halo-core-dimer vertex is ig .

The self-energy of the h field is given by a one-loop diagram, (Fig. S1)

$$\Sigma(p) = i(ig)^2 \int \frac{d^4q}{(2\pi)^4} iD(p-q) iG_\phi(q) = -4\pi i g^2 \int \frac{d^4q}{(2\pi)^4} \frac{f_a\left(\frac{1}{4}(\mathbf{p}-\mathbf{q})^2 - p_0 + q_0 - i\epsilon\right)}{q_0 - \frac{\mathbf{q}^2}{2m_\phi} + i\epsilon}. \quad (\text{S7})$$

Closing the contour in the lower half-plane, we find

$$\Sigma(p) = -4\pi g^2 \int \frac{d\mathbf{q}}{(2\pi)^3} f_a \left(-p_0 + \frac{1}{4}(\mathbf{p}-\mathbf{q})^2 + \frac{\mathbf{q}^2}{2m_\phi} \right). \quad (\text{S8})$$

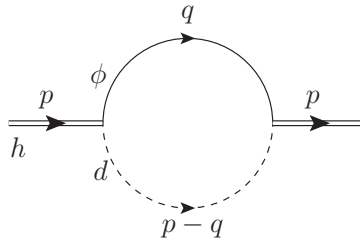


FIG. S1. The self-energy of the halo nucleus. The dash line in the loop is the dimer propagator, while the solid line is the propagator of the core.

Performing a shift $\mathbf{q} \rightarrow \mathbf{q} + \frac{m_\phi}{m_h} \mathbf{p}$, we then get

$$\Sigma(p) = -4\pi g^2 \int \frac{d\mathbf{q}}{(2\pi)^3} f_a \left(-p_0 + \frac{\mathbf{p}^2}{2m_h} + \frac{\mathbf{q}^2}{2\mu} \right), \quad (\text{S9})$$

where

$$\mu = \frac{2m_\phi}{m_h} \quad (\text{S10})$$

is the reduced mass of the core-dimer system.

The full inverse propagator of the halo is then

$$G_h^{-1}(p) = Z_h \left(p_0 - \frac{\mathbf{p}^2}{2m_h} + B_0 \right) + 4\pi g^2 \int \frac{d\mathbf{q}}{(2\pi)^3} f_a \left(-p_0 + \frac{1}{2m_h} \mathbf{p}^2 + \frac{\mathbf{q}^2}{2\mu} \right). \quad (\text{S11})$$

The integral over \mathbf{q} is quadratically divergent in the UV. We assume it is regularized by e.g., a momentum cutoff or by dimensional regularization. We use the on-shell renormalization scheme, where the following two conditions are imposed:

$$G_h^{-1}(p_0, \mathbf{0}) \Big|_{p_0=-B} = 0, \quad (\text{S12})$$

$$\frac{\partial}{\partial p_0} G_h^{-1}(p_0, \mathbf{0}) \Big|_{p_0=-B} = 1, \quad (\text{S13})$$

which means

$$Z_h(B_0 - B) + 4\pi g^2 \int \frac{d\mathbf{q}}{(2\pi)^3} f_a(B_{\mathbf{q}}) = 0, \quad (\text{S14})$$

$$Z_h - 4\pi g^2 \int \frac{d\mathbf{q}}{(2\pi)^3} f'_a(B_{\mathbf{q}}) = 1, \quad (\text{S15})$$

where

$$B_{\mathbf{q}} = B + \frac{\mathbf{q}^2}{2\mu}, \quad (\text{S16})$$

and the function f_a is defined as in Eq. (S5).

From Eq. (S15) one can derive the beta function for the running of the coupling g . Noting that $Z = g^2/g_0^2$, we find

$$g_0^2 = \frac{g^2}{1 + 4\pi g^2 \int \frac{d\mathbf{q}}{(2\pi)^3} f'_a(B_{\mathbf{q}})}. \quad (\text{S17})$$

Differentiating g_0 with respect to the the UV cutoff in the integral, we find the beta function (7).

S2. CHARGE RADIUS

The charge form factor of the halo nucleus is

$$F(\mathbf{k}) = Z_h + \Gamma(k, p), \quad (\text{S18})$$

where $\Gamma(k, p)$ is given by the Feynman diagram in Fig. S2 at the kinematic point

$$k = (0, \mathbf{k}), \quad p = \left(-B + \frac{\mathbf{k}^2}{8m_h}, \mathbf{0} \right). \quad (\text{S19})$$

We now compute the Feynman diagram in Fig. S2. Using the Feynman rules we find

$$\begin{aligned} \Gamma(k, p) &= (ig)^2 \int \frac{d^4 q}{(2\pi)^4} iG_\phi \left(q - \frac{k}{2} \right) iG_\phi \left(q + \frac{k}{2} \right) iD(p - q) \\ &= ig^2 \int \frac{d^4 q}{(2\pi)^4} \frac{D \left(-B + \frac{\mathbf{k}^2}{8m_h} - q_0, -\mathbf{q} \right)}{\left(q_0 - \varepsilon_{\mathbf{q} - \frac{\mathbf{k}}{2}} + i\epsilon \right) \left(q_0 - \varepsilon_{\mathbf{q} + \frac{\mathbf{k}}{2}} + i\epsilon \right)}, \end{aligned} \quad (\text{S20})$$

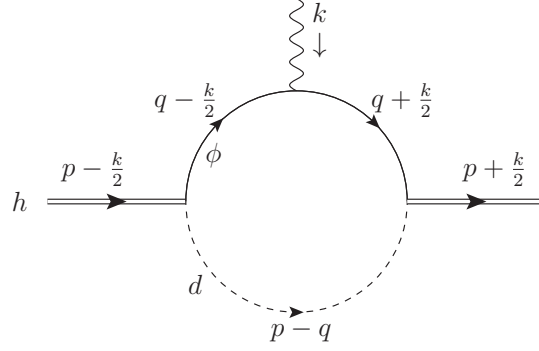


FIG. S2. The Feynman diagram that determines the charge form factor of the halo nucleus.

where $\varepsilon_{\mathbf{q}} = \mathbf{q}^2/(2m_\phi)$. Performing integral by closing the contour in the lower half-plane, one finds

$$\Gamma(k, p) = g^2 \int \frac{d\mathbf{q}}{(2\pi)^3} \frac{1}{\varepsilon_{\mathbf{q}-\frac{k}{2}} - \varepsilon_{\mathbf{q}+\frac{k}{2}}} \left[D \left(-B + \frac{\mathbf{k}^2}{8m_h} - \varepsilon_{\mathbf{q}-\frac{k}{2}}, -\mathbf{q} \right) - D \left(-B + \frac{\mathbf{k}^2}{8m_h} - \varepsilon_{\mathbf{q}+\frac{k}{2}}, -\mathbf{q} \right) \right]. \quad (\text{S21})$$

Using Eq. (S4), we have

$$F(\mathbf{k}) = Z_h + 4\pi g^2 \int \frac{d\mathbf{q}}{(2\pi)^3} \frac{m_\phi}{\mathbf{q} \cdot \mathbf{k}} \left[f_a \left(B_{\mathbf{q}} + \frac{\mathbf{k}^2}{4m_\phi m_h} - \frac{\mathbf{q} \cdot \mathbf{k}}{2m_\phi} \right) - f_a \left(B_{\mathbf{q}} + \frac{\mathbf{k}^2}{4m_\phi m_h} + \frac{\mathbf{q} \cdot \mathbf{k}}{2m_\phi} \right) \right]. \quad (\text{S22})$$

To order k^0 we have

$$F(0) = Z_h - 4\pi g^2 \int \frac{d\mathbf{q}}{(2\pi)^3} f'_a(B_{\mathbf{q}}) = 1. \quad (\text{S23})$$

where we have used Eq. (S15). This is just the statement that the total charge is equal to 1 in our normalization.

Expanding Eq. (S21) to second order in \mathbf{k} , we then find the charge radius from $F(\mathbf{k}) = 1 - \frac{1}{6} \langle r_c^2 \rangle k^2 + O(k^4)$:

$$\langle r_c^2 \rangle = \frac{4\pi g^2}{m_\phi m_h} \int \frac{d\mathbf{q}}{(2\pi)^3} \left[\frac{3}{2} f''_a(B_{\mathbf{q}}) + \frac{\mathbf{q}^2}{6\mu} f'''_a(B_{\mathbf{q}}) \right], \quad (\text{S24})$$

which can be written as

$$\langle r_c^2 \rangle = \frac{4g^2}{\pi} \frac{A^{1/2}}{(A+2)^{5/2}} \frac{1}{B} f_c \left(\frac{1}{(-a)\sqrt{B}} \right), \quad (\text{S25})$$

where

$$f_c(\beta) = \int_1^\infty dy \sqrt{y-1} \left[3f''_a(y) + \frac{2}{3}(y-1)f'''_a(y) \right] \Big|_{a=-1/\beta} \quad (\text{S26})$$

Integrating by part, this can be reduced into the form

$$f_c(\beta) = - \int_1^\infty dy \frac{f'_a(y)|_{a=-1/\beta}}{\sqrt{y-1}} = \int_1^\infty dy \frac{1}{2\sqrt{y(y-1)}(\sqrt{y}+\beta)^2} \quad (\text{S27})$$

Evaluating the integral, one obtains Eq. (11). The result for the charge radius also coincides with the value obtained from a sum rule for the dipole strength function, computed in Section S4.

S3. NEUTRON RADIUS

A. Effective coupling of the dimer to the “neutron-number photon”

The two diagrams contributing to the effective coupling of the dimer to the “neutron-number photon” are depicted in Fig. S3. They sum up to

$$\Gamma_{dd\gamma}(k, p) = i^2 \int \frac{d^4q}{(2\pi)^4} iG\left(\frac{p}{2} - q - \frac{k}{2}\right) iG\left(\frac{p}{2} - q + \frac{k}{2}\right) iG\left(\frac{p}{2} + q\right) + (q \rightarrow -q). \quad (\text{S28})$$

Performing the integral over q_0 , this becomes

$$\Gamma_{dd\gamma}(k, p) = \int \frac{d\mathbf{q}}{(2\pi)^3} \frac{2}{\left(p_0 - \frac{\mathbf{p}^2}{4} - \mathbf{q}^2 - \frac{\mathbf{k}^2}{8}\right)^2 - \frac{1}{4}\left(k_0 - \frac{\mathbf{p}\cdot\mathbf{k}}{2} + \mathbf{q}\cdot\mathbf{k}\right)^2}. \quad (\text{S29})$$

Expanding to quadratic order in \mathbf{k} and k_0 , one can write the result in terms of the three Galilean invariant quantities

$$P_0 = p_0 - \frac{\mathbf{p}^2}{4}, \quad K_0 = k_0 - \frac{\mathbf{p}\cdot\mathbf{k}}{2}, \quad k = |\mathbf{k}|, \quad (\text{S30})$$

as

$$\Gamma_{dd\gamma}(k, p) = \Gamma_0(P_0) + k^2\Gamma_1(P_0) + K_0^2\Gamma_2(P_0), \quad (\text{S31})$$

where

$$\Gamma_0(P_0) = \int \frac{d\mathbf{q}}{(2\pi)^3} \frac{2}{(P_0 - \mathbf{q}^2)^2} = \frac{1}{4\pi} \frac{1}{\sqrt{-P_0}}, \quad (\text{S32})$$

$$\Gamma_1(P_0) = \int \frac{d\mathbf{q}}{(2\pi)^3} \left[\frac{1}{2} \frac{1}{(P_0 - \mathbf{q}^2)^3} + \frac{1}{6} \frac{\mathbf{q}^2}{(P_0 - \mathbf{q}^2)^4} \right] = -\frac{5}{384\pi} \frac{1}{(-P_0)^{3/2}}, \quad (\text{S33})$$

$$\Gamma_2(P_0) = \frac{1}{2} \int \frac{d\mathbf{q}}{(2\pi)^3} \frac{1}{(P_0 - \mathbf{q}^2)^4} = \frac{1}{128\pi} \frac{1}{(-P_0)^{5/2}}. \quad (\text{S34})$$

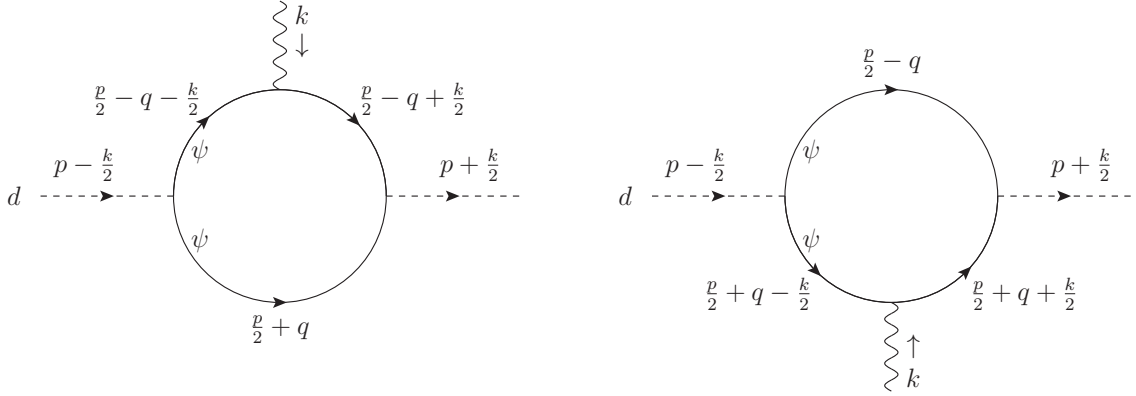


FIG. S3. The diagrams contributing to the effective coupling of a “neutron-number photon” to the dimer field.

B. Calculation of the neutron radius

We imagine that there exists a gauge boson that couples to the neutrons outside the core, but not to the core. The “neutron form factor” receives a contribution from the Feynman diagram in Fig. S4, and defined by

$$F_n(\mathbf{k}) = 2Z_h + \Gamma_n(k, p), \quad (\text{S35})$$

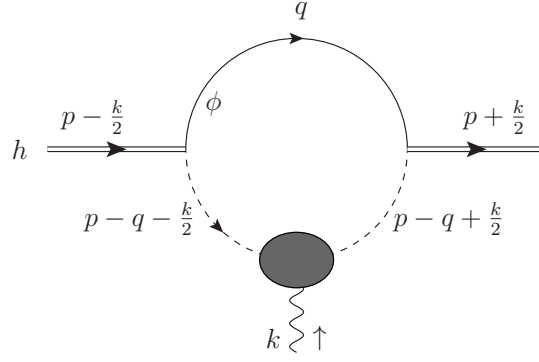


FIG. S4. The Feynman diagram that contributes to the neutron form factor of the halo nucleus.

where $\Gamma_n(k, p)$ is given by

$$\Gamma_n(k, p) = ig^2 \int \frac{d^4q}{(2\pi)^4} G_\phi(q) D\left(p - q - \frac{k}{2}\right) \Gamma_{dd\gamma}(k, p - q) D\left(p - q + \frac{k}{2}\right) \quad (\text{S36})$$

at the kinematic point (S19). Here $\Gamma_{dd\gamma}$ is the effective vertex of the coupling of the dimer to the “neutron-number photon.” This vertex has been evaluated in Sec. S3 A to second order in the photon momentum to

$$\Gamma_{dd\gamma}(k, p) = \frac{1}{4\pi} \left[\frac{1}{\sqrt{-P_0}} - \frac{5}{96} \frac{\mathbf{k}^2}{(-P_0)^{3/2}} + \frac{1}{32} \frac{K_0^2}{(-P_0)^{5/2}} \right], \quad (\text{S37})$$

where $P_0 = p_0 - \mathbf{p}^2/4$, $K_0 = k_0 - \frac{1}{2}\mathbf{p} \cdot \mathbf{k}$.

Integrating over the q_0 , closing the contour in the lower half-plane, one picks up the pole from the core propagator $G_\phi(q)$

$$\Gamma_n(k, p) = g^2 \int \frac{d\mathbf{q}}{(2\pi)^3} D\left(p - q - \frac{k}{2}\right) \Gamma_{dd\gamma}(k, p - q) D\left(p - q + \frac{k}{2}\right) \Big|_{q_0 = \frac{1}{2m_\phi} \mathbf{q}^2}. \quad (\text{S38})$$

At the kinematic point (S19), the neutron form factor of the halo nucleus is, to quadratic order in \mathbf{k} ,

$$F_n(\mathbf{k}) = 2Z_h + 4\pi g^2 \int \frac{d\mathbf{q}}{(2\pi)^3} \left[\frac{1}{\sqrt{B_{\mathbf{q}}}} + \left(-\frac{5}{96} + \frac{1}{16m_h} \right) \frac{\mathbf{k}^2}{B_{\mathbf{q}}^{3/2}} + \frac{1}{128} \frac{(\mathbf{k} \cdot \mathbf{q})^2}{B_{\mathbf{q}}^{5/2}} \right] \\ \times \left[\frac{1}{(\sqrt{B_{\mathbf{q}}} - \frac{1}{a})^2} - \frac{m_\phi}{16m_h} \frac{\mathbf{k}^2}{(\sqrt{B_{\mathbf{q}}} - \frac{1}{a})^3 \sqrt{B_{\mathbf{q}}}} + \frac{1}{64} \frac{(2\sqrt{B_{\mathbf{q}}} - \frac{1}{a})(\mathbf{q} \cdot \mathbf{k})^2}{(\sqrt{B_{\mathbf{q}}} - \frac{1}{a})^4 B_{\mathbf{q}}^{3/2}} \right]. \quad (\text{S39})$$

Recalling Eq. (S15), we find that $F_n(0)$ becomes

$$F_n(0) = 2 \left[Z_h - 4\pi g^2 \int \frac{d\mathbf{q}}{(2\pi)^3} f'(B_{\mathbf{q}}) \right] = 2, \quad (\text{S40})$$

which is the total “neutron number” of the halo nucleus. Computing $F_n(\mathbf{k})$ to order \mathbf{k}^2 , we find the neutron radius,

$$\langle r_n^2 \rangle = \frac{g^2}{\pi B} \left(\frac{A}{A+2} \right)^{3/2} \left[f_n(\beta) + \frac{A}{A+2} f_c(\beta) \right], \quad (\text{S41})$$

where $f_c(\beta)$ is as in Eq. (11), and

$$f_n(\beta) = \int dy \frac{\sqrt{y-1}}{2y^{3/2}(\sqrt{y} + \beta)^2} \quad (\text{S42})$$

Taking the integral, one obtains Eq. (13).

S4. E1 DIPOLE STRENGTH FUNCTION

To find the $E1$ dipole strength function, one needs to evaluate the Feynman diagrams, one of which is drawn on Fig. S5

$$iG_{JJ}(\omega) = (Ze)^2 (ig)^2 \int \frac{d^4q}{(2\pi)^4} iG_\phi(q) \frac{\mathbf{q}}{m_\phi} iG_\phi(q+\omega) \frac{\mathbf{q}}{m_\phi} iG_\phi(q) iD(p-q) + (\omega \rightarrow -\omega), \quad (\text{S43})$$

where $\omega = (\omega, \mathbf{0})$. Closing the contour in the lower half-plane, the imaginary part comes from the pole in $G(q+\omega)$.

$$\begin{aligned} \text{Im } G_{JJ}(\omega) &= (Ze)^2 \frac{g^2}{m_\phi^2 \omega^2} \int \frac{d\mathbf{q}}{(2\pi)^3} \mathbf{q}^2 \text{Im } D\left(\omega - B - \frac{\mathbf{q}^2}{2m_\phi}, -\mathbf{q}\right) \\ &= -(Ze)^2 \frac{4\pi g^2}{m_\phi^2 \omega^2} \int \frac{d\mathbf{q}}{(2\pi)^3} \mathbf{q}^2 \frac{\sqrt{\omega - B - \frac{\mathbf{q}^2}{2\mu}}}{\omega - B - \frac{\mathbf{q}^2}{2\mu} + \frac{1}{a^2}} \theta\left(\omega - B - \frac{\mathbf{q}^2}{2\mu}\right). \end{aligned} \quad (\text{S44})$$

Evaluating the integral one finds

$$\text{Im } G_{JJ}(\omega) = -(Ze)^2 \frac{3g^2}{8} \frac{(2\mu)^{5/2}}{m_\phi^2} \frac{(\omega - B)^2}{\omega^2} f_{E1}\left(\frac{1}{(-a)\sqrt{\omega - B}}\right), \quad (\text{S45})$$

with the function $f_{E1}(x)$ defined in Eq. (30). From this one obtains Eq. (29).

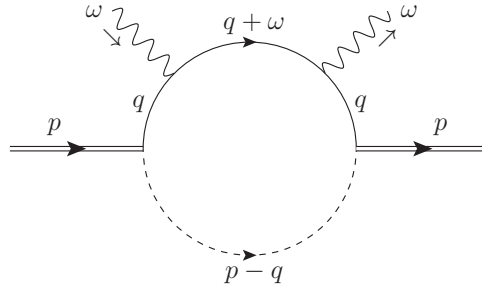


FIG. S5. The Feynman diagram determining the $E1$ dipole strength function. A second diagram obtained by reversing the direction of momentum flow on the two photon lines contributes to G_{JJ} but not to its imaginary part when $\omega > 0$.

S5. RELATIONSHIPS BETWEEN VARIOUS MEAN SQUARE RADII

Let \mathbf{r}_c denote the position of the core, and \mathbf{r}_1 and \mathbf{r}_2 those of the two neutrons. Assume that the center of mass is at the origin,

$$A\mathbf{r}_c + \mathbf{r}_1 + \mathbf{r}_2 = \mathbf{0}, \quad (\text{S46})$$

then the coordinates of every particle can be express through \mathbf{r}_c and $\mathbf{r}_{nn} = \mathbf{r}_1 - \mathbf{r}_2$:

$$\mathbf{r}_1 = -\frac{A}{2}\mathbf{r}_c + \frac{1}{2}\mathbf{r}_{nn}, \quad (\text{S47})$$

$$\mathbf{r}_2 = -\frac{A}{2}\mathbf{r}_c - \frac{1}{2}\mathbf{r}_{nn}. \quad (\text{S48})$$

Now notice that $\langle \mathbf{r}_c \cdot \mathbf{r}_{nn} \rangle = 0$ due to the symmetry of the ground-state wavefunction of the halo with respect to exchanging \mathbf{r}_1 and \mathbf{r}_2 , one can derive relationships between different mean-square radii. For example

$$\langle r_n^2 \rangle = \langle r_1^2 \rangle = \frac{A^2}{4} \langle r_c^2 \rangle + \frac{1}{4} \langle r_{nn}^2 \rangle \Rightarrow \langle r_{nn}^2 \rangle = 4 \langle r_n^2 \rangle - A^2 \langle r_c^2 \rangle. \quad (\text{S49})$$

Analogously

$$\langle r_m^2 \rangle = \frac{1}{A+2} (A\langle r_c^2 \rangle + \langle \mathbf{r}_1^2 \rangle + \langle \mathbf{r}_2^2 \rangle) = \frac{2}{A+2} \langle r_n^2 \rangle + \frac{A}{A+2} \langle r_c^2 \rangle, \quad (\text{S50})$$

$$\langle r_{cn}^2 \rangle = \frac{1}{2} [\langle (\mathbf{r}_1 - \mathbf{r}_c)^2 \rangle + \langle (\mathbf{r}_2 - \mathbf{r}_c)^2 \rangle] = \langle r_n^2 \rangle + (A+1)\langle r_c^2 \rangle, \quad (\text{S51})$$

where we used Eq. (S46) to derive the second relation.